



# Adsorption and Kinetic Studies on Sequestering Effect of Porous Biodegradable Biochar Obtained from Pig-Bone on Hexavalent Chromium from Aqueous Solution

L. Vidhya\*<sup>1</sup>, S. Vinodha\*\*<sup>2</sup>, S. J. Pradeeba\*†<sup>1</sup>, B. Jeyagowri\*<sup>1</sup>, V. Nirmaladevi\*<sup>1</sup> and N. Nithiya\*\*\*<sup>1</sup>

\*Department of Chemistry, Hindustan College of Engineering and Technology, Coimbatore-641032, Tamil Nadu, India

\*\*Department of Chemical Engineering, Jayaraj Annabackiam CSI College of Engineering, Thoothukudi-628617, Tamil Nadu, India

\*\*\*Department of Physics, Hindustan College of Engineering and Technology, Coimbatore-641032, Tamil Nadu, India

†Corresponding author: S. J. Pradeeba; pradeebasj@gmail.com

Nat. Env. & Poll. Tech.  
Website: [www.neptjournal.com](http://www.neptjournal.com)

Received: 19-08-2022

Revised: 18-10-2022

Accepted: 24-12-2022

## Key Words:

Chromium  
Pig-bone biochar  
Biosorbent  
Kinetic studies  
Isotherms

## ABSTRACT

In the current research work, the authors proposed a list of tactics to eliminate Cr (VI) with the help of pig bone biochar. The Cr (VI) was adsorbed in batches onto pig bone biochar to scrutinize the adsorption data. The studies determine the impact of adsorption dose, pH, and concentration. From the results, it was inferred that the optimum pH level was 7 for the removal of metal. The study calculated the adsorption isotherms in terms of affinity and adsorption capacity by leveraging Temkin, Langmuir and Freundlich equations. According to the reports, the Langmuir model is suitable for the adsorption data, followed by Temkin and Freundlich equations. In this model, rapid adsorption kinetic rates were observed, whereas the equilibrium state was achieved after two hours. There seems to be a perfect collation between the kinetic adsorption data and the pseudo-second-order equation. The researchers determined both Lagergren and Ho's constants. When biochar was characterized with SEM (Scanning Electron Microscope), EDX (Energy Dispersive X-ray spectrometer), and FTIR (Fourier Transform Infrared spectrometer), it was revealed that the Cr (VI) ions interacted with the isolated aggregates formed on the biosorbent surface. From the results, it can be understood that the pig bone biochar can be effectively used to eliminate chromium ions from an aqueous solution.

## INTRODUCTION

There is a tremendous increase observed in the utilization and discharge of chemicals due to rapid industrialization. Industrial effluents generally possess a huge quantity of heavy metals in them. These heavy metals get transported to other members of the ecosystem and exhibit toxicity, while they accumulate in human beings through food chain contamination. Chromium, Lead, Nickel, and Cadmium are the common toxic heavy metals that remain non-biodegradable and threaten environmental flora and fauna despite fewer concentrations (Shamaa Shroff & Varsha Vaidya 2011, Pradeeba & Sampath 2019). Having been identified as carcinogenic and mutagenic agents, these heavy metals bring imbalance in the environment. Various

industries such as paints and pigments, galvanization, metal plating, smelting and mining, textile dyeing, and leather tanning use chromium compounds in their daily purposes. So removing chromium (VI) from wastewater remains crucial before discharge. Wastewater treatment is a critical process due to various challenges associated with it, such as strict discharge regulations, costly methods of wastewater discharge, and scarce water resources. Few methods are traditionally followed in the isolation of metal ions, such as electrolysis, ion exchange, reverse osmosis, solvent extraction, precipitation, adsorption and electrochemical precipitation, and electrochemical treatment. Of these methods, the biosorption process is found to be cost-efficient and eco-friendly when it comes to metal ions isolation from contamination solution since it uses bioadsorbents (Nessim et al. 2011). The activated carbon adsorption method is deemed one of the most viable solutions to eliminate contaminants from the polluted medium. The method is also effective at low concentrations with a large surface area and high porosity (Ayaliew et al. 2014). The present study is aimed at reviewing the pig bone biochar (activated carbon) on its

ORCID details of the authors:

L. Vidhya: <https://orcid.org/0000-0001-6161-1786>

S. J. Pradeeba: <https://orcid.org/0000-0002-3737-8440>

B. Jeyagowri: <https://orcid.org/0000-0002-4252-2785>

V. Nirmaladevi: <https://orcid.org/0000-0001-8463-6185>

N. Nithiya: <https://orcid.org/0000-0003-3545-1955>

adsorption ability of Chromium (VI) ions from aqueous simulated solutions.

The study objectives are as follows; (i) amalgamate and distinguish biochar from pig bone, (ii) assess the possibility of pig bone biochar (PBBC) for the removal of Cr, (VI) from aqueous solution, (iii) evaluate the control of experimental variables on Cr (VI) adsorption onto PBBC and (iv) investigate adsorption kinetic and isotherms to identify with the mechanism of Cr (VI) removal.

## MATERIALS AND METHODS

### Preparation of Pig-Bone Biochar Adsorbent

The researcher collected the pig bones from a slaughterhouse at Navakarai village of Coimbatore, Tamil Nadu, India. After washing the pig bones extensively with deionized water, it was dried in an oven at 60°C for 24 h. Biochar was produced from these dried bones using a small-scale biochar-producing plant (Safire Scientific Company, Tamil Nadu Agriculture University, Coimbatore, Tamil Nadu, India). After crushing and drying the bones in the sun, the samples were dried in a hot air oven at 100°C for 24 h. The dehydrated material was then compressed and fed into the pyrolysis stove. The biochar sample was collected, sieved (<0.25 mm), and their notable features were determined before investigations.

### Characterization of Pig Bone Biochar

As per the literature (Shenbagavalli & Mahimairaja 2012), the sieved pig bone biochar samples were evaluated for their water-holding capacity, particle size, and zeta potential following standard methods. Further, the pig bone biochar adsorbent was also assessed for its characteristics. A particle size analyzer Horiba, SZ-100 (Japan), was used to measure the size of the pig bone biochar particles and zeta potential. As per the regulations from the American Society for Testing and Materials (ASTM 1977), the proximate and ultimate factors, for instance, ash content, volatile matter, fixed carbon content, and moisture content of the PBBC, were determined. The biochar's morphological features and elemental composition before and after Cr (VI) adsorption were determined using SEM-EDS (Scanning Electron Microscopy - Energy Dispersive Spectroscopy; Quanta FEI250, Czechoslovakia). Likewise, the biochar spectra (of Fourier transform infrared spectroscopy, FTIR) before and post-Cr (VI) adsorption were obtained using a spectrometer (Shimadzu, Model 8400S) in a diffuse reflectance moderate resolution of 8cm in KBr pellets. The researcher performed the scanning in the range of 400 to 4000  $\text{cm}^{-1}$ .

### Stock Solutions and Standards

The researcher prepared the standard stock solution using 2.828 g of  $\text{K}_2\text{Cr}_2\text{O}_7 \cdot \text{H}_2\text{O}$  (bought from Hi Media Laboratories India, (Molecular weight 294.18, 99.9% Assay) in double distilled water. The stock solution was diluted per the working concentration requirements (50–250  $\text{mg} \cdot \text{L}^{-1}$ ). All the solutions' pH values were adjusted with the help of 0.1 N HCl or 0.1 N NaOH solutions (Mohanty et al. 2014). The study used chemicals only of analytical grade.

### Analysis of Cr (VI)

Before and after the Cr (VI) got adsorbed over biochar, the Hexavalent chromium present in the solution was determined spectrophotometrically by diphenyl carbazide (Thamilarasu et al. 2011). At 540 nm, the absorbance was measured for Cr(VI) (Rajoriya & Kaur 2014) using a Shimadzu spectrophotometer. The sample concentrations were calculated with the help of a calibration graph.

### Adsorption Studies

The researcher carried out the batch adsorption experiment as given herewith. Pigbone biochar weight 0.05 g was separately placed in an Erlenmeyer flask (250 mL) (Deveci & Kar 2013). The PBBC (0.05 g) was agitated along with 25 mL of metal solution individually at  $32 \pm 10^\circ\text{C}$  briefly. After this, the solution was kept in a rotary shaker (VRN-480, GEMMY Orbit Shaker, Taiwan) to ensure a smooth blend. This was then allowed to equilibrate for two hours. Throughout the analysis, the shaking speed was maintained at 100 rpm. The samples were collected at specified time intervals, whereas the metal solution was isolated from the adsorbent by centrifuging the samples at 6,000 rpm for 5 min. At 540 nm, the supernatant was visually analyzed for residual chromium concentration using UV-Vis spectrophotometer (UV-1800 Shimadzu, Japan) once complexed with 1,5diphenylcarbazide. The study considered the following variables for the experiment (i) pH effect on adsorption capacities, (ii) dosage of PBBC (0.01 to 0.05 g), (iii) initial chromium concentration (50 to 250  $\text{mg} \cdot \text{L}^{-1}$ ) (Yang et al. 2013).

### Data Evaluation

The samples were filtered and analyzed to prevent any possible intrusion of carbon fines with the analysis. The absorbance of the supernatant solution was calculated to determine the standard solutions' residual hexavalent Cr concentration. The hexavalent chrome removal percentage (R%) was determined for every run. The experiments were conducted in triplicates, while the mean values were reported to prevent any redundancies in experimental results.

The controls for metal solutions were maintained for all the experiments. The researcher calculated the adsorption capacity at equilibrium  $q_e$ . As given herewith, the removal percentage (R %) of hexavalent chromium was determined for every run.

$$R (\%) = \frac{C_o - C_e}{C_o} * 100$$

The expression below determined the adsorption capacity for every Cr (VI) concentration at equilibrium.

$$\text{Adsorption capacity} = q_e \frac{(mg)}{(g)} = \frac{C_o - C_e}{m} * V$$

Here V denotes the volume of solution in terms of liters, whereas 'm' denotes the mass of the adsorbent utilized in grams (Hossain et al. 2012).

### Optimum Analysis of Adsorption of Cr(VI) over PBBC

According to the literature by Deveci and Kar (2013), the authors conducted batch experiments. The variables measured in the experiments were (i) pH effect on the adsorption capacities, (ii) adsorbent dosage of PBBC (0.01 to 0.05 g), and (iii) initial concentration of Cr (50 to 250 mg.L<sup>-1</sup>).

### Data Modeling

To decode the relationship between the amount of Cr (VI) ions adsorbed ( $C_e$ ) on the adsorbent surface and the equilibrium adsorption capacity ( $q_e$ ), the adsorption isotherm studies were conducted at equilibrium conditions. The researcher plotted Langmuir (equation 1), Freundlich (equation 2), and Temkin (equation 3) isotherms with the help of standard straight-line equations. While the two corresponding parameters of hexavalent chromium ions,  $C_e$  and  $Q_e$ , were determined based on the relevant graphs. According to Langmuir isotherm, monolayer sorption occurs on a homogeneous surface without interacting with the sorbed species. There seems to be a specific number of binding sites homogeneously distributed over the biosorbent surface, and it is with this theory the Langmuir isotherm equation is applied (Inyang et al. 2010). As per this theory, no interaction is found between the adsorbate and adsorbent.

Following is the linear form of the Langmuir equation.

$$\frac{C_e}{Q_e} = \frac{C_e}{Q} + \frac{1}{Qb} \quad \dots(1)$$

Where  $Q_e$  denotes the sorbent's equilibrium adsorption capacity in mg/g,  $C_e$  in mg.L<sup>-1</sup> at equilibrium indicates the concentration of metal ions. Q denotes the maximum capacity of the metal monolayer in mg.g<sup>-1</sup>, whereas b denotes the adsorption equilibrium constant in L.mg<sup>-1</sup>.

Freundlich isotherm elucidates the heavy metal adsorption by biosorbent since it is held accountable for various binding sites. Following is the notion for the adsorption isotherm model, which considers the heterogeneous adsorption on the adsorbent surface (Sukumar et al. 2014).

$$\ln q_e = \ln K_f + \frac{1}{n} \ln C_e \quad \dots(2)$$

Here,  $C_e$  denotes the equilibrium concentration of metal ion (mg.L<sup>-1</sup>), the amount of metal ion adsorbed at equilibrium (mg.g<sup>-1</sup>) is denoted by  $q_e$  (Cheng et al. 2016), n denotes the heterogeneity factor, and  $K_f$  is the Freundlich constant that is related to sorption capacity (mg.g<sup>-1</sup>). Determining  $K_f$  and n from a linear plot of log  $q_e$  against log  $C_e$  is possible.

Temkin isotherm is provided herewith as a linear equation. This model considers that the heat of adsorption (function of temperature) of almost all the molecules present in the layer gets reduced in linear relatively than logarithmic with coverage.

$$q_e = B \ln KT + B \ln C_e \quad \dots(3)$$

Where  $B_T$  denotes the Temkin constant correlated with the heat of sorption, mathematically,  $B_T = RT/b_T$  (J.mol<sup>-1</sup>) where R denotes the gas constant (8.314 J.mol<sup>-1</sup>.K<sup>-1</sup>),  $b_T$  denotes the Temkin isotherm constant, and T denotes the absolute temperature (K).  $C_e$  denotes the equilibrium concentration of a metal in solution (mg.L<sup>-1</sup>),  $q_e$  denotes the amount of Ni(II) ions sorbed onto the PBBC (mg.g<sup>-1</sup>), and  $K_T$  (L.g<sup>-1</sup>) denotes the equilibrium potential corresponding to the maximum binding energy. The researcher conducted blank experiments excluding PBBC to ensure that the sorption of Cr (VI) on the flasks' walls was negligible.

## RESULTS AND DISCUSSION

### Characterization of Biochar

Table 1 shows the results of the proximate analysis. The PBBC pH value was alkaline (7.1), like biochar from anaerobic-digested sugarcane bagasse (Janaki et al. 2013, 2014). This might be a tribute to the presence of alkali metals such as magnesium and calcium from pig bone. The PBBC moisture content was 2.20%, whereas this low moisture content denotes that the PBBC has good adsorptive capacity. The PBBC had a fixed carbon content of 60%. This denotes a high carbonization process, whereas the chances of metals getting adsorbed onto PBBC are high. The PBBC had an ash content of 29%. Zeta potential study is nothing but a measure of charge stability, and it keeps all the particle-particle interaction under control within a suspension. In Table 1, one can observe that the zeta potential of biochar



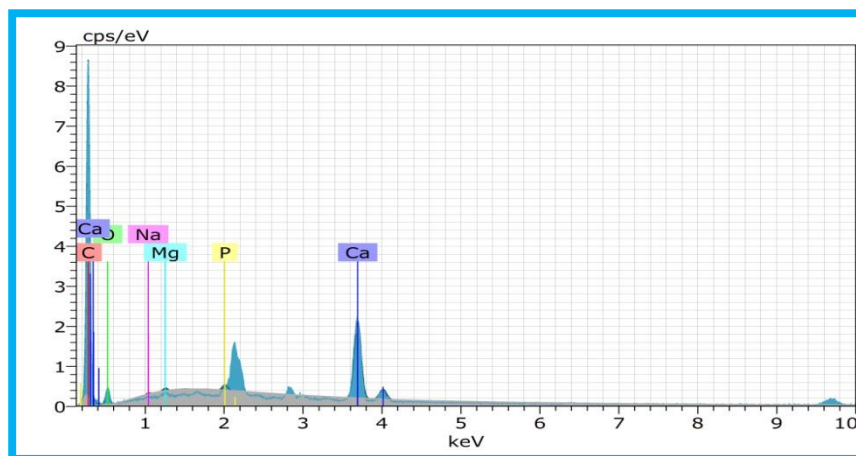


Fig. 2(b): EDAX spectra of Cr (VI) adsorbed pig bone.

The functional parameters like concentration, dosage, and pH are optimized by carrying out the trial experiments. Initial experiments are conducted with the concentration varied, and the dosage and pH kept constant. The next step is that dosage varies with concentration, keeping pH constant. Lastly, pH values are changed with concentration and dosage made constant.

### FT-IR Analysis

Several functional groups, such as sulfhydryl, alkyl, hydroxyl, aryl, carboxyl, keto, phosphate sulphonate, and amide groups, contribute to the adsorption of metal ions in biochar. Therefore, to realize the functional groups concerned

with the adsorption of Cr (VI) ions in PBBC, Fourier-transform infrared (FTIR) analysis was conducted, and the results are shown in Fig. 3(a) & 3(b). The spectra were plotted using the same scale on the transmittance axis for PBBC before and after adsorption. The FTIR spectra of the PB-BC exhibit the number of adsorption peaks, representing the composite nature. The essential changes observed in the spectrum before and after Cr (adsorption VI) onto PBBC indicated the control of various functional groups' adsorption process. The wave number  $2927.27\text{ cm}^{-1}$  to  $2923.09\text{ cm}^{-1}$  was shifted and identified as C–H stretch aldehyde groups. The transform in the peak from  $1417.15\text{ cm}^{-1}$  to  $1412.32\text{ cm}^{-1}$  depicts the presence of C–C aromatics. The peak from

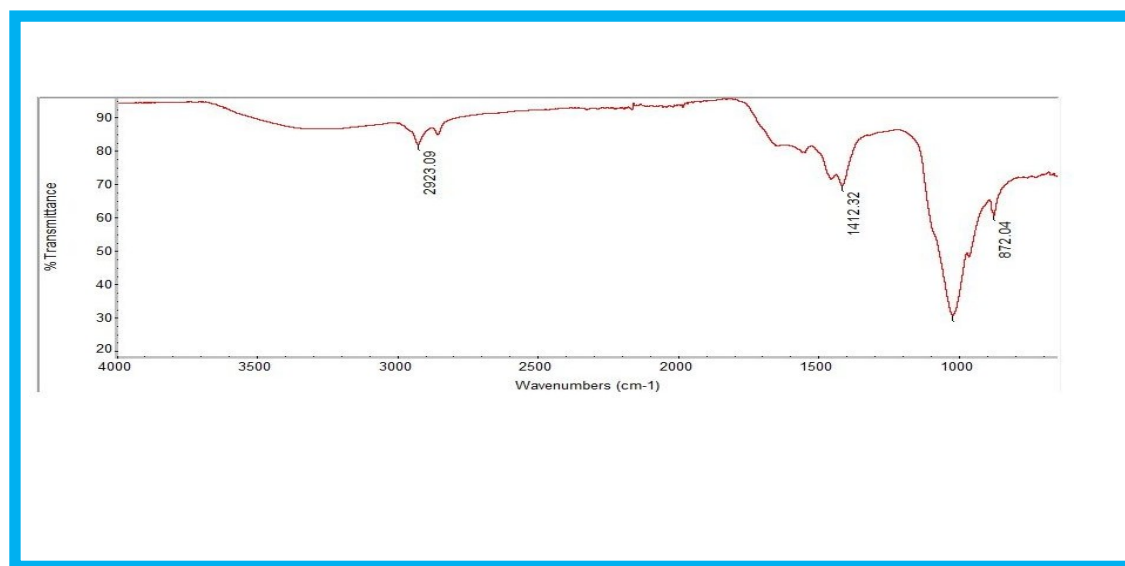


Fig. 3(a): FT-IR Spectra of blank pig bone biochar.

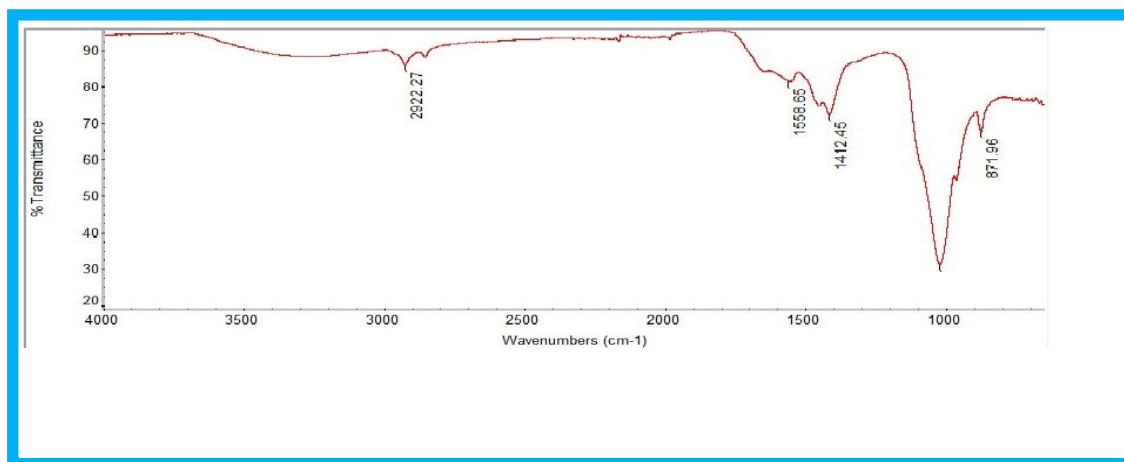


Fig. 3(b): FT-IR Spectra of Cr (VI) adsorbed pig bone biochar.

8781.96  $\text{cm}^{-1}$  to 872.04  $\text{cm}^{-1}$  depicts the bonding of C–H bending, thereby indicating the presence of an alkyl group in the adsorption process.

#### Effect of Cr (VI) Concentration

Dosage is a significant factor in the effective adsorption process. It creates a Driving force that removes all mass transfer resistance of metal ions between the aqueous phase and the solid (Shanmugapriya et al. 2013). The effect of initial Cr (VI) concentration (50 to 250  $\text{mg.L}^{-1}$ ) with the optimized parameters (0.05 g of biochar, pH 7.0) was investigated. Fig. 4(a) shows the results. There was a slight decrease observed (0.4–2%) in the removal percentage when the Cr (VI) (50 to 250  $\text{mg.L}^{-1}$ ) concentration was increased. The increased sorption at lower concentrations might be attributed to easy access to enough active sites present in biochar. At later stages, when these active sites got saturated, the sorption process slowed due to steric repulsion between solute molecules, thus reducing the removal capacity. Cadmium adsorption was also investigated in an earlier study (Mao et al. 2011) on peanut husk biochar by Cheng et al. (2016).

#### Effect of Adsorbent Dosage

Dosage is the main parameter in the sorption process since it evaluates the system's adsorbent-adsorbate equilibrium (Kumar et al. 2013). So the optimum dosage was finalized through experimentation with different doses (0.01–0.05 g) of PBBC, and the results of such experiments are showcased in Fig. 4(b) respectively. The figure shows no significant change in the removal capacity of Cr (VI) because of PBBC dosage since more than 99% removal was observed in almost all the dosages. The presence of more active sites and adsorptive surfaces present in the PBBC led to high

adsorption. The experiment results can be relied on since the literature (Arivoli et al. 2012) cited an increase in the level of Cr (VI) adsorption onto biochar prepared from oily seeds of *Pistacia terebinthus* L.

#### Effect of pH

As per Fig. 4(c), there seems to be a change in the percent removal of metal ions in the entire range of pH values from the experiments conducted. The pH of the solution remains an important parameter since it influences the interface between adsorbate and adsorbent by altering the surface charge (Pandian et al. 2014). Further, the degree of ionization of materials in the solution is also influenced by pH value. So, PBBC measuring 0.05 g was added to 100 mL of Cr (VI) (100  $\text{mg.L}^{-1}$ ) at different pH values (2–8), while Fig. 4(c) showcases the results of this experiment. One can understand that Cr and Ni get sorbed at all pH ranges (2–8) with a removal capacity of <88%. In the case of chromium, the adsorption at neutral pH (7) was found to be 99.75%, while in the case of Ni, it was 99.88%. As per the study conducted earlier (Zavvar & Seyedi 2011), the maximum adsorption at pH 7 might be attributed to the negative charge on the surface in an alkaline medium. Further, the protonation of amine and carboxyl functional groups in the PBBC adsorbent might have played an important role here. Altogether this resulted in strong electrostatic attraction between chromate ions and PBBC in chromium solution.

Further, nickelate ions and PBBC also got a similar attraction in nickel solutions. According to Janaki et al. (2014), the rivalry between  $\text{OH}^-$  ion and the chromate or nickelate ions threatens the neutral pH. This threat results in high consumption of chromium or nickel. So, the next sets of experiments were conducted at pH 7. In other

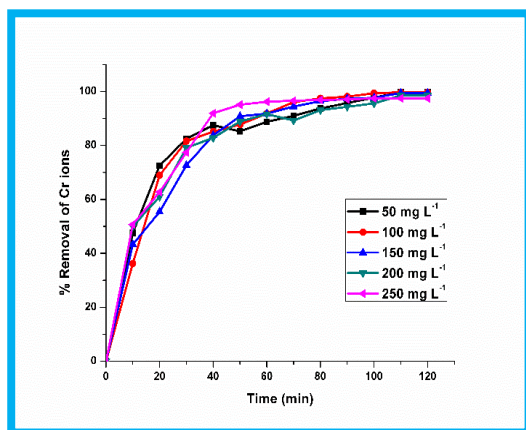


Fig. 4(a): Effect of Concentration.

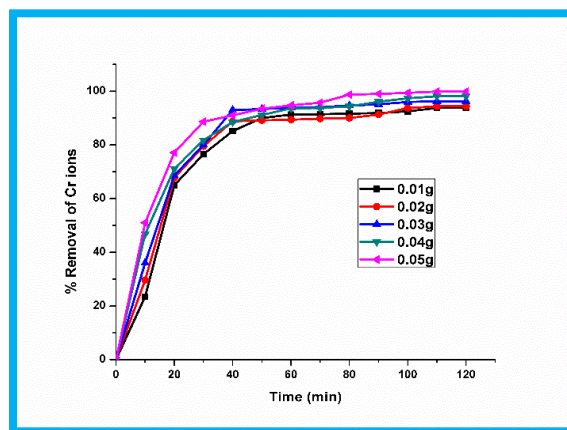


Fig. 4(b): Effect of Adsorbent Dosage.

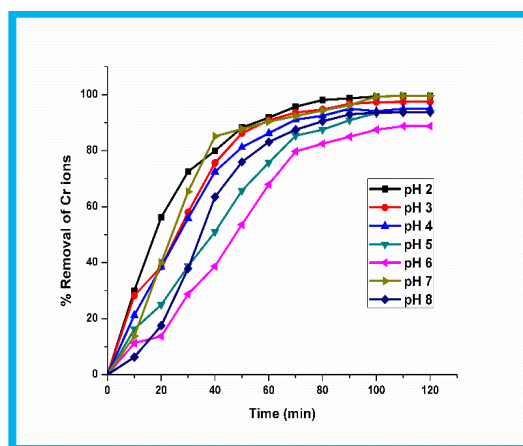


Fig. 4(C): Effect of pH.

terms, the deprotonation of the carboxylic group in acidic pH (3-6) would have mildly reduced the adsorption of Cr (VI) onto PBBC. In line with this, scenarios like increased concentration of  $\text{OH}^-$  ion in pH8, competition between  $\text{OH}^-$  ion and chromate ions or nickelate ions or in alkaline solutions may hinder the interface between PBBC and Cr (VI) ions.

The results infer that Cr (VI) adsorption may be adapted to a pH value prism dependent on PBBC features. The biochar contains cellulose, lignin, tannins, and polysaccharides which may enter into a binding reaction with Cr (VI) ions (Soheil et al. 2016) and reported similar results for cadmium adsorption onto peanut husk biochar.

### Data Modeling of Isotherms

The Langmuir isotherm denotes the development of monolayer coverage of adsorbate on the adsorbent surface. Further, one can also observe the constant nature of sorption

energy. The sites seem energetically equal without any interface between adsorbed molecules on adjacent sites (Dada et al. 2012). According to the results, an appropriate fitness is found in the case of linear equations that assess the adsorption of Cr (VI) ions onto PBBC, compared with the Langmuir equation (Pradeeba et al. 2022). Further, the maximum adsorption capacity ( $Q_e$ ) of PBBC for Chromium (VI) was found to be  $259.55 \text{ mg} \cdot \text{g}^{-1}$ . The study mentioned that the adsorbent with a high  $Q_e$  value is accepted in wastewater treatment. The relationship is more linear because the correlation coefficient value  $R^2$  is closer to 1 (Chromium  $R^2 = 0.9936$ ). So, the adsorption of Cr (VI) onto PBBC is found to have been suitable with the Langmuir isotherm equation (Fig. 5). The biochar adsorption capacity has few differences due to structural, functional differences and also due to the presence of polysaccharides in raw materials, preparation conditions, and proximate characteristics. To ensure the favorability of the adsorption process, it is possible

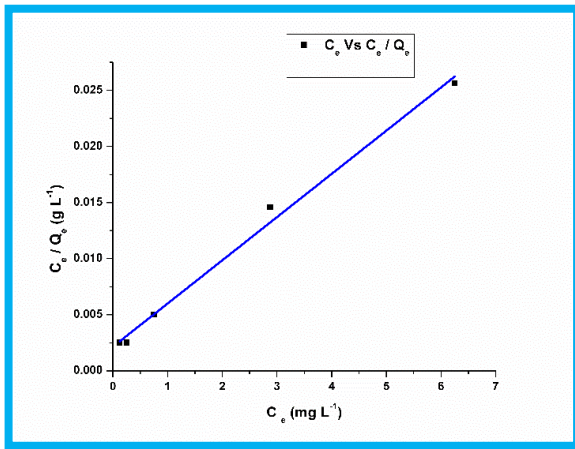


Fig. 5: Langmuir isotherm of concentration.

to explain the equilibrium parameter,  $R_L$ , and the separation factor. The following equation was used to calculate it (Dada et al. 2012).

$$R_L = 1/(1 + bC_0)$$

Table 2: Isotherm model constants for Cr (VI)ion adsorption onto PBBC.

Isotherm models	Parameters	PBBC
Langmuir model	$q_m(\text{mg.g}^{-1})$	259.55
	$K_L(\text{L.mg}^{-1})$	1.788
	$R^2$	0.99
Freundlich model	$K_f(\text{mg.g}^{-1})(\text{L.mg}^{-1})^{1/n}$	137.41
	$N$	2.72
	$R^2$	0.91
Temkin model	$K_T$	28.177
	$B_T$	46.74
	$R^2$	0.98

Where  $C_0(\text{mg.L}^{-1})$  denotes the initial concentration of metal ions,  $R_L$  value denotes either the isotherm shape is unfavorable ( $R_L > 1$ ), linear ( $R_L = 1$ ), favorable ( $0 < R_L < 1$ ), or reversible ( $R_L = 0$ ). In the current research, the  $R_L$  values (0.009-0.005) for chromium ions and (0.005-0.001) for nickel ions inferred that the adsorption of ions upon PBBC is favorable when the values lie in the range of 0 and 1. The  $R_L$

Table 3: Adsorption kinetic model constants for Cr (VI) adsorption onto PBBC.

Kinetic models	Parameters	Initial concentration [ $\text{mg.L}^{-1}$ ]				
		PBBC				
		50	100	150	200	250
PPseudo first order	$q_e(\text{exp})(\text{mg.g}^{-1})$	49.8750	99.7500	149.2500	197.1250	243.7500
	$q_e(\text{calc})(\text{mg.g}^{-1})$	31.7062	82.8083	136.7362	169.7926	145.8930
	$K_1(\text{min}^{-1})$	-0.0311	-0.0430	-0.0419	-0.0393	-0.0503
	$R^2$	0.9545	0.9403	0.9909	0.9306	0.9158
PPseudo second order	$q_e(\text{exp})(\text{mg.g}^{-1})$	49.8750	99.7500	149.2500	197.1250	243.7500
	$q_e(\text{max})(\text{mg.g}^{-1})$	52.3836	108.8068	163.5461	208.5315	260.4999
	$k_2(\text{g mg}^{-1} \text{min}^{-1})$	0.0023	0.0009	0.0005	0.0005	0.0006
	$R^2$	0.9934	0.9886	0.9878	0.9928	0.9930
	H	0.1221	0.0967	0.0875	0.1131	0.1443

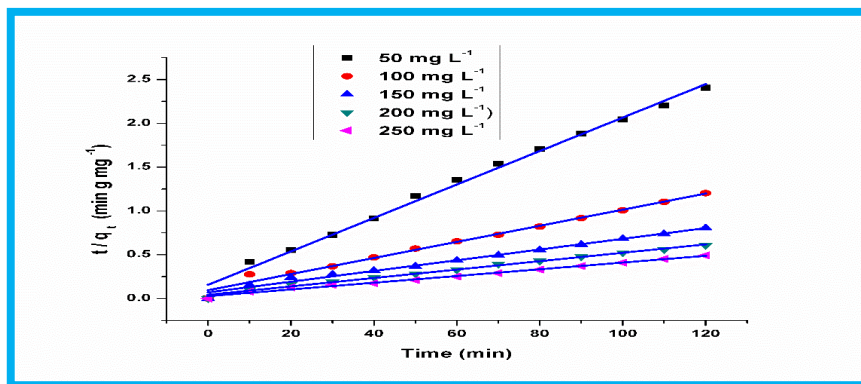


Fig. 6: Pseudo II order kinetic model for concentration.



is near 0 and is grateful to the pore diffusion sorption effect. The  $R_L$  values attained were in the range of 0 and 1. This assured the proceedings of a favorable adsorption process (Pradeeba et al. 2022).

Freundlich adsorption isotherm was attained by drawing a plot  $\ln C_e$  versus  $\ln Q_e$  in the adsorption of Ni (II) and Cr (VI) ions on PBBC. The  $K_f$  and  $n$  values were determined from the intercept and slope of the plot of  $\log C_e$  vs.  $\log Q_e$  and are shown in Table 2.

As per Table 2, the  $K_f$  values generally denote the control in adsorption capacity. The value of  $n > 1$  (or)  $1/n$  in the range of 1 and 10 infers the adsorption condition to be favorable. High adsorption co-efficient  $K_f$  values were found for Chromium (137.4072) and Nickel (144.649) on PBBC. Higher values of  $K_f$  denote that the saturation time for the adsorption of Ni and Cr ions was attained rapidly. It's a gratitude to the high affinity of PBBC towards adsorbate. In the case of Nickel ions, the values of  $1/n$  were around  $3.081 \text{ (mg.L}^{-1}\text{)}$ , and in the case of Chromium ions. It was  $2.728 \text{ (mg.L}^{-1}\text{)}$ . Based on the values attained for  $K_f$  and  $1/n$ , one can infer that PBBC is highly efficient in removing Ni or Cr ions. For Cr, the correlation coefficient value was 0.9084, and for Ni, it was 0.8206. The Tempkin isotherm evaluated the adsorption potentials of the sorbent for Cr(VI) adsorption onto the PBBC plot for sorbate. The sorption heat of molecules in the layer reduces linearly mainly because of sorbate and sorbent contacts. Table 2 shows the results along with correlation coefficients ( $R^2$ ). For Chromium (V), the correlated coefficient value was ( $R^2=0.988537$ ). The Tempkin isotherm model seemed to have good fitness for the data (Pradeeba & Sampath 2022). But of the three adsorption isotherm models under investigation, i.e., Langmuir, Freundlich, and Temkin isotherms, the Langmuir model seems appropriate for sorption data. In contrast, the value was high and remained the best fit.

### Adsorption Kinetic Models

The kinetic models are generally utilized to detail the efficacy of adsorption, associated mechanisms, and adsorbate effectiveness. So, the study used equilibrium data and investigated two kinetic models to scrutinize the adsorption mechanisms of Ni and Cr, as given herewith. Lagergren proposed a pseudo-first-order kinetic model. The adsorption rate constants and their correlation coefficients ( $R^2$ ) were determined from the curves. Table 3 shows the summary of this analysis.

From the experimental kinetic data, a low correlation coefficient was observed for the pseudo-first-order kinetic model. Fig. 6 showcases the second-order model for Chromium (VI). This proves to be a not-so-good fit

for the model. In other terms, the correlation coefficient value of the pseudo-second-order model ( $R^2=0.99$ ) was close to unity. This denotes that the pseudo-second-order model was the best fit than the pseudo-first-order model. Adding to the above, the  $q_e$  theoretical values calculated from the pseudo-second-order model were close to that of the experimental values of  $q_e$ . These outcomes denote the kinetic analysis results, i.e., the chemisorption processes control the adsorption rate (Pradeeba & Sampath 2022). The results align with earlier studies investigating the adsorption of Ni (II) and Zn (II) onto chitosan following pseudo-second-order kinetics. The pseudo-second-order kinetic equation seems to be the best-fit model in the current study.

### CONCLUSION

There was an effective removal of (>99%) of Cr (VI) observed in an aqueous solution by PBBC. The removal of Cr (VI) was heavily influenced by pH, i.e., at pH7, the maximum removal was noted. There was an increase in the adsorption of Cr (VI) on PBBC with an increase in the dose and contact time of the adsorbent. There was a decrease in the adsorption efficiency of Cr (VI) on PBBC when the initial Cr (VI) concentration was increased. Based on the kinetic studies, it can be established that the adsorption of Cr (VI) ions followed the pseudo-second-order model. At the same time, the equilibrium data had the best fit with the Langmuir isotherm. The results infer that PBBC is an efficient and cost-effective adsorbent that can remove Cr (VI) from an aqueous solution. Further, PBBC can be recycled to reduce contamination and environmental pollution.

### REFERENCES

- American Society for Testing and Materials (ASTM), USA., 1977.
- Arivoli, S., Marimuthu, V., Ravichandran, T. and Hema, M. 2012. Kinetic, equilibrium, and mechanistic studies of nickel adsorption on a low-cost activated referncalcite powder. *Indian J. Sci. Res. Tech.*, 1: 41-49.
- Ayaliew, A.W., Nigus, G.H. and Hayelom, D.B. 2014. Removal of hexavalent chromium from tannery wastewater using activated carbon primed from sugarcane bagasse: adsorption/desorption studies. *Am. J. Appl. Chem.*, 2(6): 128-135.
- Cheng, Q., Huang, Q., Khan, S., Liu, Y., Liao, Z. and Ligy, Y.S. 2016. Adsorption of Cd by peanut husks and peanut husk biochar from aqueous solution. *Ecol. Eng.*, 87: 240-245.
- Dada, A.O., Olalekan, A.P., Olatunya, A.M. and Dada, O. 2012. Langmuir, Freundlich, Temkin, and Dubinin-Radushkevich isotherm studies of equilibrium sorption of  $Zn^{2+}$  onto phosphoric acid modified rice husk. *IOSR J. Appl. Chem.*, 3(1): 38-45.
- Deveci, H. and Kar, Y. 2013. Adsorption of hexavalent chromium from aqueous solutions by bio-chars obtained during biomass pyrolysis. *J. Ind. Eng. Chem.*, 19(1): 190-196.
- Gonen, F. and Onalan, F. 2016. Adsorptive removal behaviour of procion MX-R dye from SRDW by chitosan. *Appl. Ecol. Environ. Res.*, 14(1): 77-98.

- Hossain, M.A., Hao Ngo, H., Guo, W.S. and Nguyen, T.V. 2012. Removal of copper from water by adsorption onto banana peel as bioadsorbent. *Int. J. Geomate.*, 2(2): 227-234.
- Inyang, M., Gao, B., Pullammanappalli, P., Ding, W. and Zimmerman, A.R. 2010. Biochar from anaerobically digested sugarcane bagasse. *Bioresour. Technol.*, 101(22): 8868-8872.
- Janaki, V., Shin, M.N., Kim, S.H., Lee, K.J., Cho, M., Ramasamy, A.K., Oh, B.T. and Kamala Kannan, S. 2014. Application of polyaniline / bacterial extracellular polysaccharide nanocomposite for removal and detoxification of Cr(VI). *Cellulose*, 21: 463-472.
- Janaki, V., Oh, B.T., Shanthi, K., Lee, K.J., Ramasamy, A.K. and Kamala Kannan, S. 2013. Polyaniline/chitosan composite: An eco-friendly polymer for enhanced removal of dyes from aqueous solution. *Synth. Met.*, 162(11): 974-980.
- Kumar, M., Pal, A., Singh, J., Shashank, G., Madhu, B., Ashis, V., Pal, Y.K. and Pachouri, U.C. 2013. Removal of chromium from water effluent by adsorption onto *Vetiveria zizanioides* and *Anabaena* species. *Nat. Sci.*, 5(3): 341-348.
- Mao, J., Won, S.W., Vijayaraghavan, K. and Yun, Y.S. 2010. Immobilized citric acid-treated bacterial biosorbents for the removal of cationic pollutants. *Chem. Eng. J.*, 162(2): 662-668.
- Mohanty, S. Bal, B. and Das. A.P. 2014. Adsorption of hexavalent chromium onto activated carbon. *Austin J. Biotechnol. Bioeng.*, 1(2): 5.
- Nessim, R.B., Ahmad Bassiouny, R., Hermine Zaki, R., Madelyn Moawad, N. and Kamal Kandeel, M. 2011. Biosorption of lead and cadmium using marine algae, *Chem. Biol.*, 27(6): 579-594.
- Pandian, P., Arivoli, S., Marimuthu, V. and Peter, P.R.A. 2014. Kinetic, equilibrium and mechanistic studies of nickel adsorption on acid-activated *Ipomoea carnea* leaves. *Sch. J. Eng. Tech.*, 2: 60-67.
- Prabakaran, R. and Arivoli, S. 2012. Adsorption kinetics, equilibrium and thermodynamic studies of nickel adsorption onto *Thespesia populnea* bark as biosorbent from aqueous solutions. *Euro. J. App. Eng. Sci. Res.*, 1(4): 134-142.
- Pradeeba, S.J. and Sampath, K. 2019. Synthesis and characterization of poly(azomethine)/ZnO nanocomposite towards photocatalytic degradation of methylene blue, malachite green, and bismarck brown., *J. Dyn. Syst. Meas. Contr.*, 1: 41.
- Pradeeba, S.J. and Sampath, K. 2022. Photodegradation, a thermodynamic and kinetic study of cationic and anionic dyes from effluents using polyazomethine/ZnO and polyazomethine/TiO<sub>2</sub> nanocomposites. *J. Optoelectr. Biomed. Mater.*, 14(3): 89-105.
- Pradeeba, S.J., Sampath, K. and Jeyagowri, B. 2022. Kinetic and adsorption isotherm modeling of photodegradation of anionic dyes using polyazomethine/titanium dioxide and polyazomethine/zinc oxide nanocomposite. *Desal. Water Treat.*, 262: 266-282.
- Rajoriya, S. and Kaur, B. 2014. Adsorptive removal of zinc from wastewater by natural biosorbents. *Int. J. Engg. Sci. Inv.*, 3(6): 60-80.
- Shamaa Shroff, K. and Varsha Vaidya, K. 2011. Effect of pre-treatments on biosorption of Ni (II) by dead biomass of *Mucor hiemalis*. *Bionano. Front.*, 11(6): 588-597.
- Shanmugapriya, A., Hemalatha, M., Scholastica, B. and Augustine, A.P.T. 2013. Adsorption studies of lead (II) and nickel (II) ions on chitosan-G-polyacrylonitrile. *Der. Pharma. Chemica.*, 5(3): 141-155.
- Shenbagavalli, S. and Mahimairaja, S. 2012. Production and characterization of biochar from different biological wastes. *Int. J. Plant Agric. Sci.*, 2: 2231-4490.
- Soheil, S.D., Raziye, Z.M. and Javad, M. 2016. Removal of Ni (II) and Zn (II) from aqueous solutions using chitosan. *Arch. Hyg. Sci.*, 5: 47-55.
- Sukumar, C., Gowthami, G., Nitya, R. Janaki, V., KamalaKannan, S. and Shanthi, K. 2014. Significance of co-immobilized activated carbon and *Bacillus subtilis* on the removal of Cr (VI) from aqueous solutions. *Environ. Earth Sci.*, 72: 839-847.
- Thamilarasu, P., Sivakumar, P. and Karunakaran, K. 2011. Removal of Ni (II) from aqueous solutions by adsorption onto *Cajanus cajan* L. Milsp seed shell-activated carbons. *Indian J. Chem. Technol.*, 18: 414-420.
- Yang, Z.H., Xiong, S., Wang, B., Li, Q. and Yang, W.C. 2013. Cr (III) adsorption by sugarcane pulp residue and biochar. *J. Cent. South Univ.*, 20: 1319-1325.
- Zavvar, M.H. and Seyedi, S.R. 2011. Nettle ash is a low-cost adsorbent for the removal of nickel and cadmium from wastewater. *Int. J. Environ. Sci. Tech.*, 8: 195-202.